

# High-Content Screening of Thai Medicinal Plants Reveals *Boesenbergia rotunda* Extract and its Component Panduratin A as Anti-SARS-CoV-2 Agents

**Phongthon Kanjanasirirat**

Excellence Center for Drug Discovery (ECDD), Faculty of Science, Mahidol University, Bangkok 10400 Thailand

**Ampa Suksatu**

Department of Microbiology, Faculty of Science, Mahidol University, Bangkok 10400 Thailand

**Suwimon Manopwisedjaroen**

Department of Microbiology, Faculty of Science, Mahidol University, Bangkok 10400 Thailand

**Bamroong Munyoo**

Excellence Center for Drug Discovery (ECDD), Faculty of Science, Mahidol University, Bangkok 10400 Thailand

**Patoomratana Tuchinda**

Department of Chemistry, Faculty of Science, Mahidol University, Bangkok 10400 Thailand

**Kedchin Jearawuttanakul**

Excellence Center for Drug Discovery (ECDD), Faculty of Science, Mahidol University, Bangkok 10400 Thailand

**Sawinee Seemakhan**

Excellence Center for Drug Discovery (ECDD), Faculty of Science, Mahidol University, Bangkok 10400 Thailand

**Sitthivut Charoensutthivarakul**

School of Bioinnovation and Bio-based Product Intelligence, Faculty of Science, Mahidol University, Bangkok 10400 Thailand

**Patomporn Wongtrakoongate**

Department of Biochemistry, Faculty of Science, Mahidol University, Bangkok 10400 Thailand

**Noppawan Rangkasenee**

Excellence Center for Drug Discovery (ECDD), Faculty of Science, Mahidol University, Bangkok 10400 Thailand

**Supaporn Pitiporn**

Chao Phraya Aphaiphubet Hospital, Prachin Buri 25000 Thailand

**Neti Waranuch**

Department of Pharmaceutical Technology, Faculty of Pharmaceutical Sciences, Naresuan University,  
Phitsanulok 65000 Thailand

**Napason Chabang**

School of Bioinovation and Bio-based Product Intelligence, Faculty of Science, Mahidol University,  
Bangkok 10400 Thailand

**Phisit Khemawoot**

Chakri Naruebodindra Medical Institute, Faculty of Medicine Ramathibodi Hospital, Mahidol University,  
Samutprakarn 10540 Thailand

**Somchai Chutipongtanate**

Department of Pediatrics, Faculty of Medicine Ramathibodi Hospital, Mahidol University, Bangkok  
10400 Thailand

**Suradej Hongeng**

Department of Pediatrics, Faculty of Medicine Ramathibodi Hospital, Mahidol University, Bangkok  
10400 Thailand

**Suparerk Borwornpinyo (✉ [bsuparerk@gmail.com](mailto:bsuparerk@gmail.com))**

Excellence Center for Drug Discovery (ECDD), Faculty of Science, Mahidol University, Bangkok 10400  
Thailand

**Arunee Thitithanyanont (✉ [arunee.thi@mahidol.edu](mailto:arunee.thi@mahidol.edu))**

Department of Microbiology, Faculty of Science, Mahidol University, Bangkok 10400 Thailand

---

**Research Article**

**Keywords:** SARS-CoV-2, COVID-19, Antivirals, Panduratin A, Boesenbergia rotunda, High-content screening

**Posted Date:** June 3rd, 2020

**DOI:** <https://doi.org/10.21203/rs.3.rs-32489/v1>

**License:**  This work is licensed under a Creative Commons Attribution 4.0 International License.

[Read Full License](#)

---

**Version of Record:** A version of this preprint was published at Scientific Reports on November 17th, 2020.  
See the published version at <https://doi.org/10.1038/s41598-020-77003-3>.

## Abstract

Since December 2019, the emergence of severe acute respiratory syndrome coronavirus-2 (SARS-CoV-2) has caused severe pneumonia, a disease named COVID-19, that became pandemic and created an acute threat to public health. The effective therapeutics are in urgent need. Here, we developed a high-content screening for the antiviral candidates using fluorescence-based SARS-CoV-2 nucleoprotein detection in Vero E6 cells coupled with plaque reduction assay. Among 122 Thai natural products, we found that *Boesenbergia rotunda* extract and its phytochemical compound, panduratin A, exhibited the potent anti-SARS-CoV-2 activity. Treatment with *B. rotunda* extract and panduratin A after viral infection drastically suppressed SARS-CoV-2 infectivity in Vero E6 cells with IC<sub>50</sub> of 3.62 µg/mL (CC<sub>50</sub> = 28.06 µg/mL) and 0.81 µM (CC<sub>50</sub>=14.71 µM), respectively. Also, the treatment of panduratin A at the pre-entry phase inhibited SARS-CoV-2 infection with IC<sub>50</sub> of 5.30 µM (CC<sub>50</sub>=43.47 µM). Our study demonstrated, for the first time, that panduratin A exerts the inhibitory effect against SARS-CoV-2 infection at both pre-entry and post-infection phases. Since *B. rotunda* is a culinary herb generally grown in China and Southeast Asia, its extract and the purified panduratin A may serve as the promising candidates for therapeutic purposes with economic advantage during COVID-19 situation.

## Introduction

In December 2019, multiple severe pneumonia cases emerged in Wuhan, Hubei, China.<sup>1</sup> The causative agent was identified as a novel coronavirus, which was scientifically named severe acute respiratory syndrome coronavirus 2 (SARS-CoV-2). The World Health Organization (WHO) called the disease caused by this virus as coronavirus disease 19 or COVID-19. With the vast and rapid spreading, the virus became pandemic in a short period, causing a severe outbreak in 216 countries and territories around the world. As of May 21, 2020, the total confirmed cases of COVID-19 were more than 4,900,000, with more than 320,000 deaths globally.<sup>2</sup> This catastrophic situation highlighted the urgent need of the entire population for the effective and affordable antiviral therapeutics to fight against the dreadful disease.

SARS-CoV-2 is an enveloped, positive-sense, single-stranded RNA virus of *Coronaviridae* family. This virus was categorized as a member of *Betacoronavirus* genus alongside severe acute respiratory syndrome coronavirus (SARS-CoV) and Middle East respiratory syndrome coronavirus (MERS-CoV). Usually, most human cases of coronavirus infection are mild or asymptomatic. However, the outbreak of SARS-CoV in 2003,<sup>3,4</sup> MERS-CoV in 2014,<sup>5</sup> and SARS-CoV-2 rang the alarm bell of the global public health crisis. Currently, there are no specific drugs for the treatment of COVID-19. All drug options are based on the treatment of the related viruses, such as SARS-CoV, MERS-CoV, influenza virus, Ebola virus, and HIV-1. Accordingly, several FDA-approved drugs with a broad therapeutic window serve as potential candidates for COVID-19 treatment.<sup>6,7</sup> The most promising repurposed drugs included chloroquine/hydroxychloroquine,<sup>8–10</sup> favipiravir,<sup>11</sup> lopinavir/ritonavir,<sup>12</sup> and remdesivir.<sup>13,14</sup> However, the degree of efficacy and the severe side effects of these drugs were still under controversy.<sup>15–17</sup> Apart from FDA-approved drugs, natural product-based medicines are gained much attention. The use of Thai

traditional herbs, particularly their phytochemicals, has been reported to exert broad-spectrum activities as the anticancer, anti-inflammatory, antioxidant therapeutics, and antivirals.<sup>18–21</sup> This suggests their potential as the anti-SARS-CoV–2 candidates.

Phytochemicals and plant-derived extracts are ideal places to find a promising drug component against coronavirus.<sup>22</sup> Several phytochemicals are currently under investigation for their applications in treating SARS-CoV–2, as many research groups have recently reported their studies on the potential use of these materials. One of the studies led by Jin Z. *et al.*,<sup>23</sup> demonstrated that the main protease ( $M^{pro}$ ) of SARS-CoV–2, a prospective drug target involved in the viral replication and transcription, can be targeted by Shikonin, a common plant-derived naphthoquinone. Further study on the molecular docking showed a reasonable docking pose indicating that Shikonin could bind to the substrate pocket.<sup>23</sup> Khan SA, *et al.*,<sup>24</sup> employed the computational based methods to identify chymotrypsin-like protease inhibitors ( $3CL^{Pro}$ ) from FDA-approved antivirals and natural compounds library. Three antiviral drugs (Remdesivir, Saquinavir, and Darunavir) and two natural compounds (flavone and coumarin derivatives) were identified as potential inhibitors for  $3CL^{Pro}$  of the coronavirus. Another study on the structure of SARS-CoV–2  $3CL^{Pro}$  has revealed several potential phytochemical flavonoids, including myricitrin and licoleafol, as inhibitors against this enzyme using the predicted 3D structure.<sup>25</sup> Although these results are encouraging, there are not enough *in vitro* data to further confirm the benefit and potential of these materials.

In recent years, cell-based phenotypic methods combining with high-content imaging technology have dramatically changed the landscape of the drug discovery process. This technique has proven to be valuable and influential in discovering molecules with desired biological functions in a relevant cell-based setting.<sup>26</sup> Due to the urgent scenario and the prospective potential of phytochemicals as an alternative treatment against novel coronavirus as demonstrated by a relevant study on their anti-SARS-CoV activities,<sup>22,27</sup> it has prompted us to develop, for the first time, a high-content screening platform to investigate the *in vitro* potential of locally obtained natural extracts and compounds found in Thai medicinal plants against SARS-CoV–2.

From this rationale, we established a high-content screening platform for the antiviral drug candidates by using a fluorescence-based technique. A total of 122 of the extracts and purified compounds derived Thai medicinal plants were screened. The extracts and compounds with the high antiviral potency were further evaluated by dose-response analysis and plaque reduction assay. In the end, this study demonstrated that *Boesenbergia rotunda* extract and its phytochemical, panduratin A, were the promising candidates for a novel treatment against COVID–19.

## Results

### High-content screening of Thai natural compounds reveals four candidates with potential anti-SARS-CoV–2 activities

The high-content imaging screening system was developed and optimized in Vero E6 cells infected with SARS-CoV-2 at 25TCID<sub>50</sub>. At 48 hrs after infection, the infected cells were evaluated by fluorescence analysis with the primary antibody specific to NP of SARS-CoV, which was able to cross-react with NP protein of SARS-CoV-2. The neutralizing serum from COVID-19 patient (the positive control) completely blocked SARS-CoV-2 infectivity (*Figure 1a and 1b*). Hydroxychloroquine and ivermectin, two FDA-approved drugs with reported anti-SARS-CoV2 activities in *vitro* and in clinical trials [8–10, 29, 30], were included as reference drugs to validate our screening system. Hydroxychloroquine showed a potent antiviral effect against SARS-CoV-2 with IC<sub>50</sub> of 5.08 μM. Besides, this drug had less cytotoxic with CC<sub>50</sub> >100 μM (*Figure 1c*). Ivermectin demonstrated the anti-SARS-CoV-2 activity with IC<sub>50</sub> of 12.68 μM. However, its therapeutic window was narrow with CC<sub>50</sub> of 31.68 μM (*Figure 1d*). The production of the infectious virion, as measured by plaque reduction assay, confirmed SARS-CoV-2 suppression following hydroxychloroquine and ivermectin treatments (*Figure 1e and 1f*). This finding pointed out the high efficacy of hydroxychloroquine in the inhibition of SARS-CoV-2 infectivity in Vero E6 cells and encouraged to use this drug as the validated control in further experiments.

Subsequently, we performed the high-content screening of Thai natural products, consisting of medicinal plant extracts and phytochemical compounds, to search for the new and promising anti-SARs-CoV-2 candidates. A total of 122 of the crude extracts and the purified compounds derived from Thai natural products were investigated. Four candidates consisting of two extracts (at 10 g/mL) of *Boesenbergia rotunda* (fingerroot) and *Zingiber officinale* (ginger), and two purified compounds (at 10 M), i.e., andrographolide and panduratin A exhibited 99.9% inhibitory activities (*Figure 1g and 1h*). Interestingly, panduratin A is the purified compound derived from *B. rotunda*. This finding encouraged us to look for *Andrographis paniculata* and 6-Gingerol, the extract and the purified compound counterpart of andrographolide and *Z. officinale*, respectively. We found that *A. paniculata* extract (at 10 g/mL) had moderate inhibitory activity, while 6-Gingerol (at 10 M) had a mild effect against SARS-CoV-2 (*Figure 1g and 1h*). This result suggested further evaluation of these medicinal plant extracts and phytochemical compounds in a dose-response manner.

## Dose-response relationship of six selected candidates at post-infectious phase

From the initial screening, three pairs of Thai medicinal plant extracts and their purified compounds (*Figure 1g and 1h*) were selected to further examine for antiviral potentials. In this part, the post-treatment approach was followed, in which two-fold dilutions of the extracts or the compounds were added into the cell culture after 2 hrs viral infection and maintained for the 48 hrs period. Thereafter, the culture supernatants were harvested, and the cells were fixed and stained with anti-SARS-CoV NP mAb and Alexa Fluor 488-labeled secondary antibody (*Figure 2a*). Hydroxychloroquine at the IC<sub>50</sub> concentration (5.08 μM; as showed in *Figure 1c*), together with the neutralizing serum, served as the positive controls of the experiment (*Figure 2b*). Overall, each of six candidates exhibited a dose-response relationship. The extract of *A. paniculata* and its purified compound, andrographolide, showed the potent antiviral effect

with  $IC_{50}$  of 68.06  $\mu$ g/mL ( $CC_{50} > 100 \mu$ g/mL) and 6.58  $\mu$ M ( $CC_{50} = 27.77 \mu$ M), respectively (Figure 2c and 2f). The anti-SARS-CoV–2 potential of *Z. officinale* extract exhibited  $IC_{50}$  of 29.19  $\mu$ g/mL ( $CC_{50} = 52.75 \mu$ g/mL) (Figure 2d); however, its purified compound 6-Gingerol had lower potency with  $IC_{50} > 100 \mu$ M ( $CC_{50} > 100 \mu$ M) (Figure 2g). Among six selected candidates, the *B. rotunda* extract and its purified compound, panduratin A, exhibited very potent anti-SARS-CoV–2 activity with  $IC_{50}$  of 3.62  $\mu$ g/mL ( $CC_{50} = 28.06 \mu$ g/mL) and 0.81  $\mu$ M ( $CC_{50} = 14.71 \mu$ M), respectively (Figure 2e and 2h). Analyses of viral output by plaque assay (Figure 2i–2n) were consistent with the high-content screening results (Figure 2c–2h).. The absolute inhibition of the infectious virion production in the post-treatment approach was observed in *A. paniculata* extract (100  $\mu$ g/mL), andrographolide (12.5  $\mu$ M), *B. rotunda* extract (12.5  $\mu$ g/mL), and panduratin A (5  $\mu$ M). Collectively, *B. rotunda* extract and its purified compound panduratin A had higher anti-SARS-CoV–2 activities than other candidates.

## Anti-SARS-CoV–2 effect of *Boesenbergia rotunda* extract and panduratin A at the pre-entry phase

*B. rotunda* extract and panduratin A had very potent anti-SARS-CoV–2 activities in the post-infection phase. To extend this impact, it was interesting to know whether or not *B. rotunda* extract and panduratin A also interfere with the viral entry. Pre-entry treatment was carried out to address this issue (Figure 3a). In this procedure, *B. rotunda* extract and panduratin A were pre-incubated with SARS-CoV–2 at 37 °C for 1 hr before inoculation into Vero E6 cells. Viral adsorption was allowed for 2 hrs in the presence of the extract/compound. Then, the cells were washed by fresh medium to remove both unbound viral particles and the extract/compound, fresh medium was supplemented, and the cells were further cultured for 48 hrs before harvest (Figure 3a). Hydroxychloroquine (at the  $IC_{50} = 8.07 \mu$ M for pre-entry treatment; details in Supplementary Figure 1) and the neutralizing serum were used as the control to validate the feasibility and interpretability of the pre-entry treatment (Figure 3b). Interestingly, *B. rotunda* extract and panduratin A also exhibited anti-SARS-CoV–2 activities in the pre-entry phase. The  $IC_{50}$  of *B. rotunda* extract and panduratin A were 20.42  $\mu$ g/mL ( $CC_{50} > 100 \mu$ g/mL) and 5.30  $\mu$ M ( $CC_{50} = 43.47 \mu$ M), respectively (Figure 3c and 3d). Even though it was less effective than that of post-infection condition, viral output analysis demonstrated approximately five-fold reduction of the infectious virion production following treatment with *B. rotunda* extract (Figure 3e). Again, Panduratin A absolutely suppressed the infectious virion production at a high dose of 50  $\mu$ M (Figure 3f).

We also explored whether *B. rotunda* extract and panduratin A could induce the antiviral state of the cells by treating the extract/compound with the cells before viral adsorption (Supplementary Figure 2).. The results showed the same trend, but both *B. rotunda* extract and panduratin A not showing a dramatic antiviral effect in this mode.

## Discussion

In this study, the high-content imaging system, coupled with the plaque assay, was utilized for the first time to identify anti-SARS-CoV–2 agents from the Thai medicinal plant library, consisting of 114 medicinal plant extracts and 8 purified compounds (details in *Supplementary Table 1*). Among the positive hits, the crude extract of *B. rotunda* and its purified compound, panduratin A, demonstrated the most potent inhibitory effect against SARS-CoV–2 replication and infectivity with the favorable cytotoxicity profile. Interestingly, panduratin A inhibited SARS-CoV–2 infectivity and replication at both pre-entry and post-infection phases, and its antiviral activity was even more potent than hydroxychloroquine FDA-approved drug currently used for COVID–19 treatment.<sup>8–10</sup> The IC<sub>50</sub>, CC<sub>50</sub>, and the selectivity index of panduratin A and hydroxychloroquine were summarized in *Table 1*. This finding highlighted the potential implication of panduratin A as the novel anti-SARS-CoV–2 candidate for COVID–19 therapy. Nevertheless, *in vivo* study and the clinical trial are needed to assess the pharmacokinetic effect and the appropriate human dose of panduratin A before clinical use.

**Table 1. A summary of anti-SARS-CoV-2 activity (IC<sub>50</sub>), cytotoxicity (CC<sub>50</sub>), and the selectivity index (SI) of panduratin A and hydroxychloroquine.**

	IC <sub>50</sub> (mM)	CC <sub>50</sub> (mM)	SI (CC <sub>50</sub> /IC <sub>50</sub> )
<b>Post-infection</b>			
Panduratin A	0.81	14.71	18.16
Hydroxychloroquine	5.08	>100	>19.68
<b>Pre-entry</b>			
Panduratin A	5.30	43.47	8.20
Hydroxychloroquine	8.07	>100	>12.39

*Boesenbergia rotunda* (fingerroot) belongs to the ginger family (*Zingiberaceae*). This herb is widely used culinarily in China and Southeast Asia. Extracts of fingerroot rhizomes are well-known for its various pharmacological effects such as anti-allergic,<sup>31</sup> antibacterial,<sup>32,33</sup> antioxidant,<sup>34</sup> and anti-tumor activities.<sup>35,36</sup> Among the major active ingredients found in fingerroot, panduratin A, a prenylated cyclohexenyl chalcone, has been reported to possibly exhibit the antiviral activity against HIV–1 and dengue virus (DENV).<sup>37–40</sup>

Several molecular and cellular mechanisms might be employed by panduratin A to exert its effect on anti-SARS-CoV–2 activity. Using the biochemical approach, this phytochemical was demonstrated to physically bind and inhibit an HIV–1 protease<sup>37</sup> and a DENV NS2B/NS3 protease.<sup>38</sup> Also, the structure-based computational approach supported panduratin A potential as the competitive inhibitor of NS2B/NS3 of DENV2.<sup>39,40</sup> Whether this compound interacts with those proteases *in vivo* is yet to be determined. In this view, panduratin A might act as the protease inhibitor to exhibit the anti-SARS-CoV–2 effect.

Another possible mechanism of panduratin A action might have occurred through its antioxidant activity. This compound itself is a potent reducing agent and can decrease levels of reactive oxygen species

(ROS) *in vitro*.<sup>41,42</sup> Whether the ROS scavenging mechanism facilitates the attenuation of SARS-CoV–2 infection by panduratin A, similar to that observed in Japanese Encephalitis virus (JEV),<sup>43</sup> is yet to be deciphered. Further, this anti-oxidative stress might be coupled with anti-inflammatory responses widely reported for panduratin A. For example, panduratin A can reduce the expression of genes whose function is involved in inflammation.<sup>44–47</sup> Undoubtedly, therapeutic strategies aiming at the modulation of inflammation has been proposed for COVID–19 as a mean to reduce the severity of the disease.<sup>48</sup>

Besides, panduratin A was found to induce autophagy, which is vital in restricting viral replication. Nonetheless, concerns have also been raised regarding the protective role of autophagy for the evasion of host innate immunity upon viral infection.<sup>49–51</sup> Autophagic induction by panduratin A treatment in mammalian cells occurred through the activation of AMPK and inhibition of mTORC1.<sup>52,53</sup> The small molecule compound has also been shown to induce PERK/eIF2α/ATF4/CHOP pathway pertinent to endoplasmic reticulum (ER) stress. Consequently, the induction of ER stress can further facilitate autophagy.<sup>54,55</sup> Moreover, panduratin A can stimulate AMPK signaling leading to the activation of PPAR $\alpha$  and PPAR $\delta$ .<sup>56,57</sup> The induction of these transcription factor machinery can, in turn, promote autophagy.<sup>58,59</sup> Consistently, it was reported that MERS-CoV blocked the fusion of autophagosomes and lysosomes. As a result, the induction of autophagy attenuated the replication of this virus.<sup>60</sup> Interestingly, the anti-helminthic and FDA-approved drug niclosamide has recently been proposed as a potential anti-SARS-CoV–2 agent,<sup>61,62</sup> possibly through its autophagic induction mechanism.<sup>63</sup> It has yet to be elucidated whether panduratin A suppresses SARS-CoV–2 infection via the induction of autophagy, and which pathway is a direct target for this compound.

Taken together, we identified *B. rotunda* extract and its active compound, panduratin A, as the promising anti-SARS-CoV–2 agents by using the high-content imaging system coupled with the plaque reduction assay. Importantly, *B. rotunda* extract and panduratin A exhibited the potent antiviral efficacy when the treatment was performed after SARS-CoV–2 infection, with the optimal IC<sub>50</sub> (3.62 µg/mL and 0.81 µM, respectively) and the favorable cytotoxicity profile (CC<sub>50</sub> 28.06 µg/mL and 14.71 µM, respectively). Panduratin A inhibited SARS-CoV–2 infectivity in the pre-entry phase as well. The information from this present study suggested the promise of panduratin A as a single therapy, and as the combinational therapeutic with other FDA-approved agents, for the effective treatment of COVID–19. The possibility of this rationale should be further evaluated. Since *B. rotunda* is the common plant affordable and available in tropical regions, a pharmaceutically active compound derived from *B. rotunda* offers a tremendous therapeutic opportunity to fight in this bloody COVID–19 battlefield. Accordingly, we suggested panduratin A as the novel natural candidate for anti-SARS-CoV–2 infection.

## Materials And Methods

### Study design

In this *in vitro* phenotypic screening of medicinal plant extracts and phytochemicals, the experiments were performed in two approaches; pre-entry and post-infectious treatments.

The pre-entry condition was designed based on the hypothesis that a particular extract or compound could participate in direct interaction with virion and hinder viral entry into the target cells. The drugs, natural extracts, or phytochemicals were pre-incubated with the virus before the inoculation of the mixture into the cells.

For the post-treatment, this approach aimed to investigate the effect of the selected drugs, natural extract, or phytochemicals in the ability to inhibit SARS-CoV-2 infectivity once the viral adsorption has been initiated. From this rationale, the drugs, natural extracts, or phytochemicals were supplemented into the culture medium after viral infection and maintained throughout the experimental period.

## Cell culture

Vero E6 cells, African green monkey (*Cercopithecus aethiops*) kidney epithelial cells (ATCC #C1008), were used for the antiviral screening in this study. The cells were grown in Dulbecco's Modified Eagle Medium (DMEM) (Gibco, USA) with 10% fetal bovine serum (FBS) (Gibco, USA). For Vero cells (African green monkey epithelial cells), these cells were cultured in Minimum Essential Medium (MEM) (Gibco, USA) supplemented with 10% FBS and L-glutamine (Gibco, USA). All cultures were grown at 37 °C in 5% CO<sub>2</sub> atmosphere.

## Virus

SARS-CoV-2 virus (SARS-CoV-2/01/human/Jan2020/Thailand) was isolated in Vero cells from nasopharyngeal swabs of a confirmed COVID-19 patient in Thailand. The virus was propagated in Vero E6 cells by three passages to establish a high-titer stock (passage 4) and stored at -80 °C for using in all experiments. Virus titration as TCID<sub>50</sub> titer/mL was performed in the 96-well microtiter plate. Briefly, the virus stock was titrated in quadruplicate in 96-well microtiter plates on Vero E6 cells in serial dilution to obtain 50% tissue culture infectious dose (TCID<sub>50</sub>) by using the Reed Muench method.<sup>28</sup> All the experiments with live SARS-CoV-2 virus were performed at a certified biosafety level 3 facility.

## Plant materials

Plant materials in the screening study were common herbs in Thailand, and most of them were listed in Thai Herbal Pharmacopoeia 2018 (<https://bdn.go.th/th/sDetail/10/34/>). *Boesenbergia rotunda* rhizomes were purchased from suppliers in Pathum Thani, Thailand. The plant was identified and compared with depository plant materials of ECDD before starting extraction procedures.

## Extracts and compounds

The air-dried and finely powdered rhizomes of *B. rotunda* (2.5 kg) were percolated with 95% EtOH (6 L, 4 times x 7 days) at room temperature to give a crude EtOH extract (190.5 g) after solvent removal. The obtained EtOH extract was divided into two portions. Each portion was separated by VLC over Si-gel (250 g each, Merck Art. No. 7731), packing on a sintered glass funnel (i.d. 12.5 cm × packing height 4.5 cm), using EtOAc-hexanes and MeOH-EtOAc gradients as eluents, respectively. Fractions (500 mL each) were collected and combined based on their TLC behaviors to give frs. A<sub>1</sub>–A<sub>5</sub>. Fr. A<sub>4</sub> (60.1 g, eluted with 25–100% EtOAc-hexanes), after three further consecutive Si-gel CC (Si-gel: Merck, Art. No 7734, 1<sup>st</sup> CC: 20% EtOAc-hexanes; 2<sup>nd</sup> CC: 60% CH<sub>2</sub>Cl<sub>2</sub>-hexanes; 3<sup>rd</sup> CC: 10% CH<sub>3</sub>COCH<sub>3</sub>-hexanes) afforded three separated frs. B<sub>1</sub>–B<sub>3</sub>. Fr. B<sub>3</sub> (5.37 g) was further purified by Sephadex LH-20 CC (Sephadex LH-20: GE Healthcare Bio-Sciences AB, 10% MeOH-CH<sub>2</sub>Cl<sub>2</sub>), followed by recrystallization from EtOH-CH<sub>2</sub>Cl<sub>2</sub> to provide pure panduratin A (3.18 g).

## In vitro antiviral assay

A total of 1x10<sup>4</sup> Vero E6 cells were cultured in a 96-black well plate (Corning, USA) for 24 hours at 37 °C in 5% CO<sub>2</sub> atmosphere. Then, culture supernatant was discarded, and the cells were washed once with phosphate-buffered saline (PBS). In the case of post-treatment, the cells were subsequently infected with SARS-CoV-2 at 25TCID<sub>50</sub>. After viral adsorption for 2 hours at 37 °C, the cells were washed twice to remove the excessive inoculum with PBS, and the fresh culture medium (DMEM with 2% FBS) was added into the wells. Each concentration of drugs, crude extracts, or active compounds was directly inoculated into the culture medium. The cells were then maintained at 37 °C in 5% CO<sub>2</sub> incubator for 48 hours. For pre-entry treatment, the mixture of each drug, crude extract, or active compound and 25TCID<sub>50</sub> of SARS-CoV-2 was incubated at 37 °C for 1 hour before inoculating it into the cells. Similarly, viral adsorption was allowed for 2 hours. After that, the cells were washed twice with PBS, and the fresh culture medium (DMEM with 2% FBS) was added into the cells. The culture was maintained for an additional 48 hours. For the pre-treatment experiment, each concentration of drugs, crude extracts, or active compounds was directly inoculated into the cells before viral infection. After incubation at 37 °C for 1 hr, drug, crude extract or compound was removed and the cells were washed with PBS. Then, the cells were infected with SARS-CoV-2 at 25TCID<sub>50</sub>. Viral adsorption was carried out for 2 hours at 37°C followed by washing with PBS. Fresh medium (DMEM with 2% FBS) was added into the wells, and the culture was maintained for 48 hours. Positive convalescent serum (heat-inactivated at 56 °C for 30 min.) of a COVID-19 patient and anti-human IgG-FITC (sc-2456; Santa Cruz) was used as a viral inhibition positive control and negative control, respectively. The experiment was done in triplicate.

## High-content imaging system for SARS-CoV nucleoprotein detection

In each treatment condition, the cells in the 96-well plate were fixed and permeabilized with 50% (v/v) acetone in methanol on ice for 20 min. The cells were washed once with phosphate-buffered saline with 0.5% Tween® detergent (PBST) and blocked in PBST with 2% (w/v) BSA for 1 hr at room temperature. After blocking, the cells were incubated with 1:500 dilution ratio of primary antibody specific for SARS-CoV Nucleoprotein (NP) (Rabbit mAb) (Sino Biological Inc. China) for 1 hr at 37 °C. This antibody can cross-react with the NP protein of SARS-CoV–2 as well. The unbound antibody was removed by washing with PBST three times. Then, the Goat anti-Rabbit IgG (H+L) Highly Cross-Adsorbed Secondary Antibody, Alexa Fluor 488 (Thermo Fisher Scientific, USA), was used at 1:500 dilution ratio. Nuclei of the cells were stained with Hoechst dye (Thermo Fisher Scientific, USA). The fluorescent signals were detected and analyzed by the high-content imaging system (Operetta, PerkinElmer) at 40x. The percentage of the infected cells in each well was automatically obtained from 13 images per well using Harmony software (PerkinElmer) (the parameters and the analytical sequence were provided in *Supplementary Information*).

## Plaque assay

The viral output of SARS-CoV–2 was reported as the infectious titers that were determined by plaque assay. In brief, Vero cell monolayer was seeded into 6-well plate 24 hours before infection. The cells were inoculated with a serial dilution of the virus and incubated for viral adsorption for 1 hr at 37 °C. Then, the cells were overlaid with 3 mL/well of overlay medium containing MEM supplemented with 5% FBS and 1% agarose. The culture was incubated at 37 °C in 5% CO<sub>2</sub> for three days to allow plaque development. After that, plaque phenotypes were visualized by staining with 0.33% Neutral Red solution (Sigma, USA) for 5 hrs. Plaque numbers were counted as plaque-forming units per milliliter (PFUs/mL) and presented as the percentage of plaque reduction.

## Data availability

All data generated or analyzed during this study are included in this article and Supplementary Information files.

## Declarations

## ACKNOWLEDGMENTS

This study was supported by the Ramathibodi Research Cluster Grant, Faculty of Medicine Ramathibodi Hospital, and Faculty of Science, Mahidol University, Thailand. PW was financially supported by New Discovery and Frontier Research Grant (NDFR 11/2563). SoC was financially supported by the Faculty Staff Development Program of Faculty of Medicine Ramathibodi Hospital, for his research activities. SH was supported by the Ramathibodi Foundation. SB was supported by the Thailand Center of Excellence for Life Sciences (TCELS) Grant (TC-A15/63). AT was supported by the Chaophaya Abhaibhubejhr Hospital Foundation. The research project is supported by Mahidol University, Thailand.

# COMPETING INTERESTS

All authors declare no conflicts of interest.

# AUTHOR CONTRIBUTIONS

SH, SB, AT initiate the conception. PK, AS, SoC, SH, SB, AT developed the design. PK, AS, SM, BM, PT, KJ, SS performed experiments. All authors analyzed and interpreted the data. PK, AS, SoC prepared figures and tables. PK and AS wrote the first draft of the manuscript. SM, BM, PT, KJ, SS, SiC, PW, NR, SP, NW, NC, PK, SoC, SH, SB, AT revised the manuscript. SB and AT finalized the manuscript. SH contributed to the overall research strategy. All authors read and approved the final version of the manuscript to be published.

# References

1. Huang C, et al. Chronological Changes of Viral Shedding in Adult Inpatients with COVID-19 in Wuhan, China. *Clin Infect Dis.* ciaa631, DOI:10.1093/cid/ciaa631 (2020).
2. WHO. Coronavirus disease (COVID-19) outbreak situation.  
<https://www.who.int/emergencies/diseases/novel-coronavirus-2019> (accessed May 7, 2020).
3. Smith RD. Responding to global infectious disease outbreaks: lessons from SARS on the role of risk perception, communication and management. *Soc Sci Med.* 63, 3113-3123, DOI:10.1016/j.socscimed.2006.08.004 (2006).
4. Anderson RM, et al. Epidemiology, transmission dynamics and control of SARS: the 2002–2003 epidemic. *Philos Trans R Soc Lond B Biol Sci.* 359, 1091-1105, DOI:10.1098/rstb.2004.1490 (2004).
5. Al-Omari A, Rabaan AA, Salih S, Al-Tawfiq JA, Memish ZA. MERS coronavirus outbreak: Implications for emerging viral infections. *Diagn Microbiol Infect Dis.* 93, 265-285, DOI:10.1016/j.diagmicrobio.2018.10.011 (2019).
6. Lu H. Drug treatment options for the 2019-new coronavirus (2019-nCoV). *Biosci Trends.* 14, 69-71, DOI:10.5582/bst.2020.01020 (2020).
7. Sanders JM, Monogue ML, Jodlowski TZ, Cutrell JB. Pharmacologic Treatments for Coronavirus Disease 2019 (COVID-19): A Review. *JAMA.* [Online ahead of print] DOI:10.1001/jama.2020.6019 (2020).
8. Gao J, Tian Z, Yang X. Breakthrough: Chloroquine phosphate has shown apparent efficacy in treatment of COVID-19 associated pneumonia in clinical studies. *Biosci Trends.* 14, 72-73, DOI:10.5582/bst.2020.01047 (2020).
9. Yao X, et al. In Vitro Antiviral Activity and Projection of Optimized Dosing Design of Hydroxychloroquine for the Treatment of Severe Acute Respiratory Syndrome Coronavirus 2 (SARS-CoV-2). *Clin Infect Dis.* ciaa237, DOI:10.1093/cid/ciaa237 (2020).

10. Colson P, Rolain JM, Lagier JC, Brouqui P, Raoult D. Chloroquine and hydroxychloroquine as available weapons to fight COVID-19. *Int J Antimicrob Agents*. 55, 105932, doi:10.1016/j.ijantimicag.2020.105932 (2020).
11. Chen C, et al. Favipiravir versus Arbidol for COVID-19: a randomized clinical trial. *medRxiv*. Preprint posted March 27, 2020.
12. Cao B, et al. A Trial of Lopinavir-Ritonavir in Adults Hospitalized with Severe Covid-19. *N Engl J Med*. 382, 1787-1799, DOI:10.1056/NEJMoa2001282 (2020).
13. Al-Tawfiq JA, Al-Homoud AH, Memish ZA. Remdesivir as a possible therapeutic option for the COVID-19. *Travel Med Infect Dis*. 34, 101615, DOI:10.1016/j.tmaid.2020.101615 (2020).
14. Wang M, et al. Remdesivir and chloroquine effectively inhibit the recently emerged novel coronavirus (2019-nCoV) in vitro. *Cell Res*. 30, 269-271, DOI:10.1038/s41422-020-0282-0 (2020).
15. Costanzo M, De Giglio MAR, Roviello GN. SARS-CoV-2: Recent Reports on Antiviral Therapies Based on Lopinavir/Ritonavir, Darunavir/Umifenovir, Hydroxychloroquine, Remdesivir, Favipiravir and Other Drugs for the Treatment of the New Coronavirus. *Curr Med Chem*. [Online ahead of print.] DOI:10.2174/0929867327666200416131117 (2020).
16. Chen J, Liu D, Liu L, et al. A pilot study of hydroxychloroquine in treatment of patients with common coronavirus disease-19 (COVID-19). *J Zhejiang Univ (Med Sci)*. 49, 215–219, DOI:10.3785/j.issn.1008-9292.2020.03.03 (2020).
17. Cao B, Wang Y, Wen D, et al. A Trial of Lopinavir-Ritonavir in Adults Hospitalized with Severe Covid-19. *N Engl J Med*. 382, 1787-1799, DOI:10.1056/NEJMoa2001282 (2020).
18. Chusri S, Singthong P, Kaewmanee T. Antioxidant, anticancer, and cytotoxic effects of Thai traditional herbal preparations consumed as rejuvenators. *CyTA - Journal of Food*. 13, 40–48, DOI: 10.1080/19476337.2014.909885 (2015).
19. Lumlerdkij N, et al. Understanding cancer and its treatment in Thai traditional medicine: An ethnopharmacological-anthropological investigation. *J Ethnopharmacol*. 216, 259-273, DOI:10.1016/j.jep.2018.01.029 (2018).
20. Sangkitporn S, et al. Efficacy and safety of zidovudine and zalcitabine combined with a combination of herbs in the treatment of HIV-infected Thai patients. *Southeast Asian J Trop Med Public Health*. 36, 704-708 (2005).
21. Chotchoungchatchai S, Saralamp P, Jenjittikul T, Pornsiripongse S, Prathanturarug S. Medicinal plants used with Thai Traditional Medicine in modern healthcare services: a case study in Kabchoeng Hospital, Surin Province, Thailand. *J Ethnopharmacol*. 141, 193-205, DOI:10.1016/j.jep.2012.02.019 (2012).
22. Mani JS, et al. Natural product-derived phytochemicals as potential agents against coronaviruses: A review. *Virus Res*. 284, 197989, DOI:10.1016/j.virusres.2020.197989 (2020).
23. Jin Z, et al. Structure of Mpro from SARS-CoV-2 and discovery of its inhibitors. *Nature*. [Online ahead of print] DOI:10.1038/s41586-020-2223-y (2020).

24. Khan SA, Zia K, Ashraf S, Uddin R, Ul-Haq Z. Identification of chymotrypsin-like protease inhibitors of SARS-CoV-2 via integrated computational approach. *J Biomol Struct Dyn.* 1-10, DOI:10.1080/07391102.2020.1751298 (2020).
25. Ul Qamar MT, Alqahtani SM, Alamri MA, Chen LL. Structural basis of SARS-CoV-2 3CLpro and anti-COVID-19 drug discovery from medicinal plants. *J Pharm Anal.* [Online ahead of print] DOI:10.1016/j.jpha.2020.03.009 (2020).
26. Singh S, Carpenter AE, Genovesio A. Increasing the Content of High-Content Screening: An Overview. *J Biomol Screen.* 19, 640-650, DOI:10.1177/1087057114528537 (2014).
27. Islam MT, et al. Natural products and their derivatives against coronavirus: A review of the non-clinical and pre-clinical data. *Phytother Res.* [Online ahead of print] DOI:10.1002/ptr.6700 (2020).
28. Reed LJ, Muench H. A simple method of estimating fifty percent endpoints. *Am J Hyg.* 27, 493–497, DOI:10.1093/oxfordjournals.aje.a118408 (1938).
29. Caly L, Druce JD, Catton MG, Jans DA, Wagstaff KM. The FDA-approved drug ivermectin inhibits the replication of SARS-CoV-2 in vitro. *Antiviral Res.* [Online ahead of print] DOI:10.1016/j.antiviral.2020.104787 (2020).
30. Schmith VD, Zhou JJ, Lohmer LR. The Approved Dose of Ivermectin Alone is not the Ideal Dose for the Treatment of COVID-19. *Clin Pharmacol Ther.* [Online ahead of print] DOI:10.1002/cpt.1889 (2020).
31. Tewtrakul S, Subhadhirasakul S. Anti-allergic activity of some selected plants in the Zingiberaceae family. *J Ethnopharmacol.* 109, 535-538, DOI:10.1016/j.jep.2006.08.010 (2007).
32. Teethaisong Y, Pimchan T, Srisawat R, Hobbs G, Eumkeb G. *Boesenbergia rotunda* (L.) Mansf. extract potentiates the antibacterial activity of some β-lactams against β-lactam-resistant staphylococci. *J Glob Antimicrob Resist.* 12, 207-213. DOI:10.1016/j.jgar.2017.10.019 (2018).
33. Udomthanadech K, Vajrodaya S, Paisooksantivatana Y. Antibacterial properties of the extracts from some Zingibereous species in Thailand against bacteria causing diarrhea and food poisoning in human. *Int Trans J Eng Manage Appl Sci Technol.* 6, 203–13, DOI: 10.14456/itjemast.2015.4 (2015).
34. Isa NM, Abdelwahab SI, Mohan S, et al. In vitro anti-inflammatory, cytotoxic and antioxidant activities of boesenbergin A, a chalcone isolated from *Boesenbergia rotunda* (L.) (fingerroot). *Braz J Med Biol Res.* 45, 524-530, DOI:10.1590/s0100-879x2012007500022 (2012).
35. Break MKB, et al. Cytotoxic Activity of *Boesenbergia rotunda* Extracts against Nasopharyngeal Carcinoma Cells (HK1). Cardamonin, a *Boesenbergia rotunda* Constituent, Inhibits Growth and Migration of HK1 Cells by Inducing Caspase-Dependent Apoptosis and G2/M-Phase Arrest. *Nutr Cancer.* [Online ahead of print] DOI:10.1080/01635581.2020.1751217 (2020).
36. Murakami, A, Kondo, A, Nakamura, Y, Ohigashi, H, Koshimizu, K. Possible Anti-tumor Promoting Properties of Edible Plants from Thailand, and Identification of an Active Constituent, Cardamonin, of *Boesenbergia pandurata*. *Biosci. Biotech. Biochem.* 57, 1971–1973, DOI:10.1271/bbb.57.1971 (1993).

37. Cheenpracha S, Karalai C, Ponglimanont C, Subhadhirasakul S, Tewtrakul S. Anti-HIV-1 protease activity of compounds from Boesenbergia pandurata. *Bioorg Med Chem.* 14, 1710-1714. DOI:10.1016/j.bmc.2005.10.019 (2006).
38. Kiat TS, et al. Inhibitory activity of cyclohexenyl chalcone derivatives and flavonoids of fingerroot, *Boesenbergia rotunda* (L.), towards dengue-2 virus NS3 protease. *Bioorg Med Chem Lett.* 16, 3337-3340. DOI:10.1016/j.bmcl.2005.12.075 (2006).
39. Frimayanti N, Chee CF, Zain SM, Rahman NA. Design of new competitive dengue NS2B/NS3 protease inhibitors-a computational approach. *Int J Mol Sci.* 12, 1089-1100. DOI:10.3390/ijms12021089 (2011).
40. Frimayanti N, et al. Fragment-based molecular design of new competitive dengue Den2 Ns2b/Ns3 inhibitors from the components of fingerroot (*Boesenbergia rotunda*). *In Silico Biol.* 11, 29-37. DOI:10.3233/ISB-2012-0442 (2011).
41. Sohn JH, Han KL, Lee SH, Hwang JK. Protective effects of panduratin A against oxidative damage of tert-butylhydroperoxide in human HepG2 cells. *Biol Pharm Bull.* 28, 1083-1086. DOI:10.1248/bpb.28.1083 (2005).
42. Salama SM, AlRashdi AS, Abdulla MA, Hassandarvish P, Bilgen M. Protective activity of Panduratin A against thioacetamide-induced oxidative damage: demonstration with in vitro experiments using WRL-68 liver cell line. *BMC Complement Altern Med.* 13, 279. DOI:10.1186/1472-6882-13-279 (2013).
43. Zhang Y, Wang Z, Chen H, Chen Z, Tian Y. Antioxidants: potential antiviral agents for Japanese encephalitis virus infection. *Int J Infect Dis.* 24, 30-36, DOI:10.1016/j.ijid.2014.02.011 (2014).
44. Cheah SC, et al. Panduratin A inhibits the growth of A549 cells through induction of apoptosis and inhibition of NF-kappaB translocation. *Molecules.* 16, 2583-2598, DOI:10.3390/molecules16032583 (2011)
45. Cheah SC, Lai SL, Lee ST, Hadi AH, Mustafa MR. Panduratin A, a possible inhibitor in metastasized A549 cells through inhibition of NF-kappa B translocation and chemoinvasion. *Molecules.* 18, 8764-8778, DOI:10.3390/molecules18088764 (2013).
46. Kim H, et al. Inhibitory Effects of Standardized *Boesenbergia pandurata* Extract and Its Active Compound Panduratin A on Lipopolysaccharide-Induced Periodontal Inflammation and Alveolar Bone Loss in Rats. *J Med Food.* 21, 961-970, DOI:10.1089/jmf.2017.4155 (2018).
47. Choi S, Kim C, Son H, Hwang JK, Kang W. Estimation of an Appropriate Human Dose of *Boesenbergia pandurata* Extracts Based on Allometric Scaling Data of Panduratin A in Mice, Rats, and Dogs. *J Med Food.* 23, 453-458, DOI:10.1089/jmf.2019.4564 (2020).
48. Tay MZ, Poh CM, Rénia L, MacAry PA, Ng LFP. The trinity of COVID-19: immunity, inflammation and intervention [published online ahead of print, 2020 Apr 28]. *Nat Rev Immunol.* [Online ahead of print] DOI:10.1038/s41577-020-0311-8 (2020).
49. Shoji-Kawata S, Levine B. Autophagy, antiviral immunity, and viral countermeasures. *Biochim Biophys Acta.* 1793, 1478-1484, DOI:10.1016/j.bbamcr.2009.02.008 (2009).

50. Ahmad L, Mostowy S, Sancho-Shimizu V. Autophagy-Virus Interplay: From Cell Biology to Human Disease. *Front Cell Dev Biol.* 6, 155, DOI:10.3389/fcell.2018.00155 (2018).
51. Choi Y, Bowman JW, Jung JU. Autophagy during viral infection - a double-edged sword. *Nat Rev Microbiol.* 16, 341-354, DOI:10.1038/s41579-018-0003-6 (2018).
52. Lai SL, Wong PF, Lim TK, Lin Q, Mustafa MR. iTRAQ-based proteomic identification of proteins involved in anti-angiogenic effects of Panduratin A on HUVECs. *Phytomedicine.* 22, 203-212, DOI:10.1016/j.phymed.2014.11.016 (2015).
53. Lai SL, Mustafa MR, Wong PF. Panduratin A induces protective autophagy in melanoma via the AMPK and mTOR pathway. *Phytomedicine.* 42, 144-151, DOI:10.1016/j.phymed.2018.03.027 (2018).
54. Yorimitsu T, Nair U, Yang Z, Klionsky DJ. Endoplasmic reticulum stress triggers autophagy. *J Biol Chem.* 281, 30299-30304, DOI:10.1074/jbc.M607007200 (2006).
55. Cybulsky AV. Endoplasmic reticulum stress, the unfolded protein response and autophagy in kidney diseases. *Nat Rev Nephrol.* 13, 681-696, DOI:10.1038/nrneph.2017.129 (2017).
56. Kim D, Lee MS, Jo K, Lee KE, Hwang JK. Therapeutic potential of panduratin A, LKB1-dependent AMP-activated protein kinase stimulator, with activation of PPAR $\alpha/\delta$  for the treatment of obesity. *Diabetes Obes Metab.* 13, 584-593, DOI:10.1111/j.1463-1326.2011.01379.x (2011).
57. Kim MS, Pyun HB, Hwang JK. Panduratin A, an activator of PPAR $\alpha/\delta$ , suppresses the development of oxazolone-induced atopic dermatitis-like symptoms in hairless mice. *Life Sci.* 100, 45-54, DOI:10.1016/j.lfs.2014.01.076 (2014).
58. Jiao M, Ren F, Zhou L, et al. Peroxisome proliferator-activated receptor  $\alpha$  activation attenuates the inflammatory response to protect the liver from acute failure by promoting the autophagy pathway. *Cell Death Dis.* 5, e1397. DOI:10.1038/cddis.2014.361 (2014).
59. Tong L, Wang L, Yao S, et al. PPAR $\delta$  attenuates hepatic steatosis through autophagy-mediated fatty acid oxidation. *Cell Death Dis.* 10, 197, DOI:10.1038/s41419-019-1458-8 (2019).
60. Gassen NC, Niemeyer D, Muth D, et al. SKP2 attenuates autophagy through Beclin1-ubiquitination and its inhibition reduces MERS-CoV infection. *Nat Commun.* 10, 5770, DOI:10.1038/s41467-019-13659-4 (2019).
61. Jeon S, Ko M, Lee J, et al. Identification of antiviral drug candidates against SARS-CoV-2 from FDA-approved drugs. *Antimicrob Agents Chemother.* AAC.00819-20. DOI:10.1128/AAC.00819-20 (2020).
62. Pindiprolu SKSS, Pindiprolu SH. Plausible mechanisms of Niclosamide as an antiviral agent against COVID-19. *Med Hypotheses.* 140, 109765, DOI:10.1016/j.mehy.2020.109765 (2020).
63. Gassen NC, et al. Analysis of SARS-CoV-2-controlled autophagy reveals spermidine, MK-2206, and niclosamide as putative antiviral therapeutics. *bioRxiv:* 2020.2004.2015.997254 (2020).

## Figures

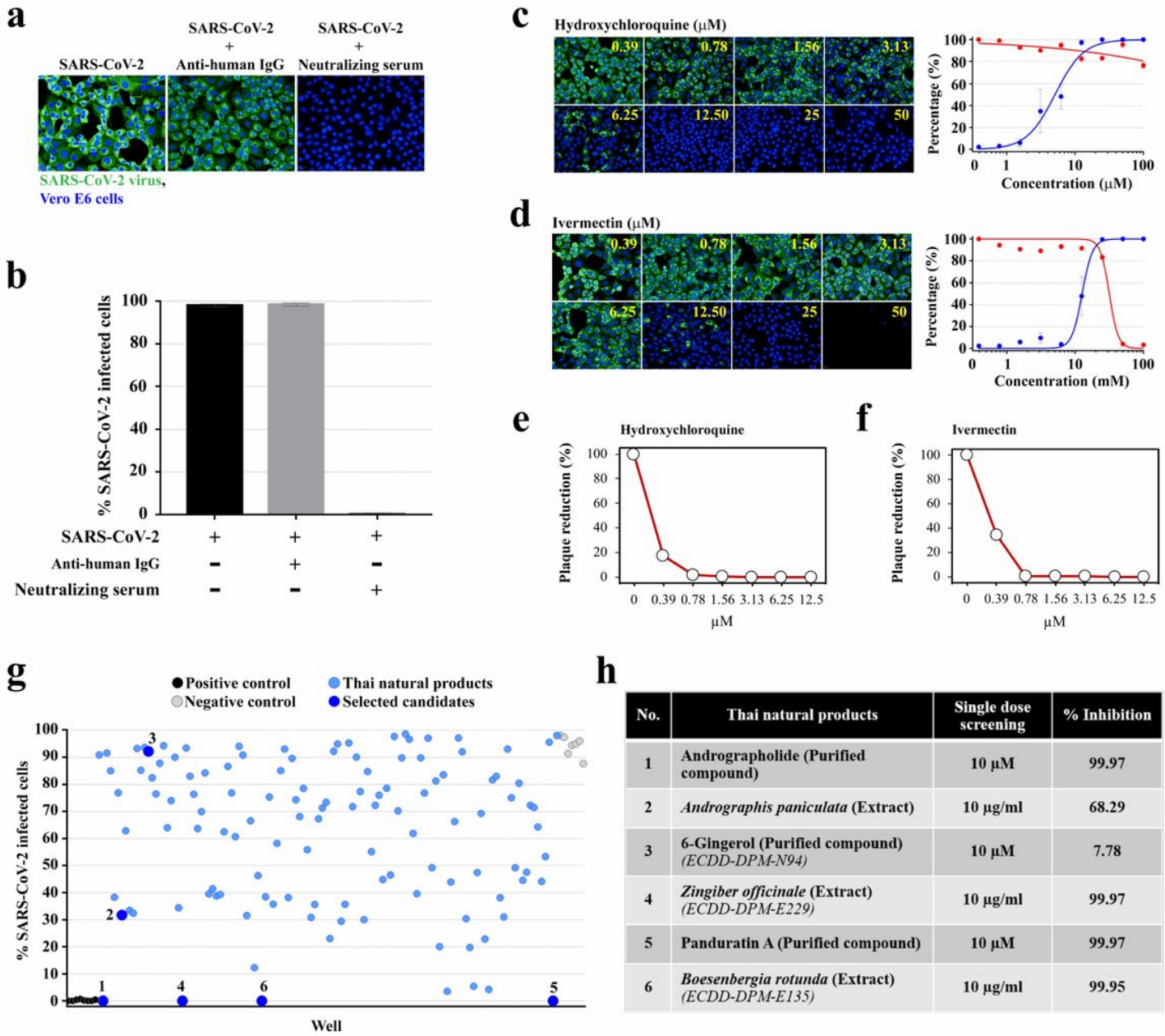


**Figure 1**

High-content anti-SARS-CoV-2 compound screening. (a). The SARS-CoV-2 (at 25TCID<sub>50</sub>) infected cells detected by high-content imaging of the control condition. Fluorescent signals: green, anti-SARS-CoV NP mAb; blue, Hoechst. (b). %infected Vero E6 of the control conditions. (c, d). The high-content images of infected cells treated with hydroxychloroquine (c) and ivermectin (d) (the left panel), and the %inhibition (red) and %cytotoxicity (blue) (the right panel) (n=3 biological replicates). (e, f). The production of infectious SARS-CoV-2 in Vero E6 cells was evaluated by plaque reduction assay after 48 hrs of hydroxychloroquine (e) and ivermectin (f) treatment (n=2 biological replicates) (g). A total of 122 Thai natural products (114 medicinal plant extracts and 8 purified compounds) were screened for anti-SARS-CoV-2 activity (n=2 technical replicates). (h). %inhibition of six selected candidates corresponding to the

number-labeled blue dots in Figure 1g. Full details of the screening results provided in Supplementary Table 1.

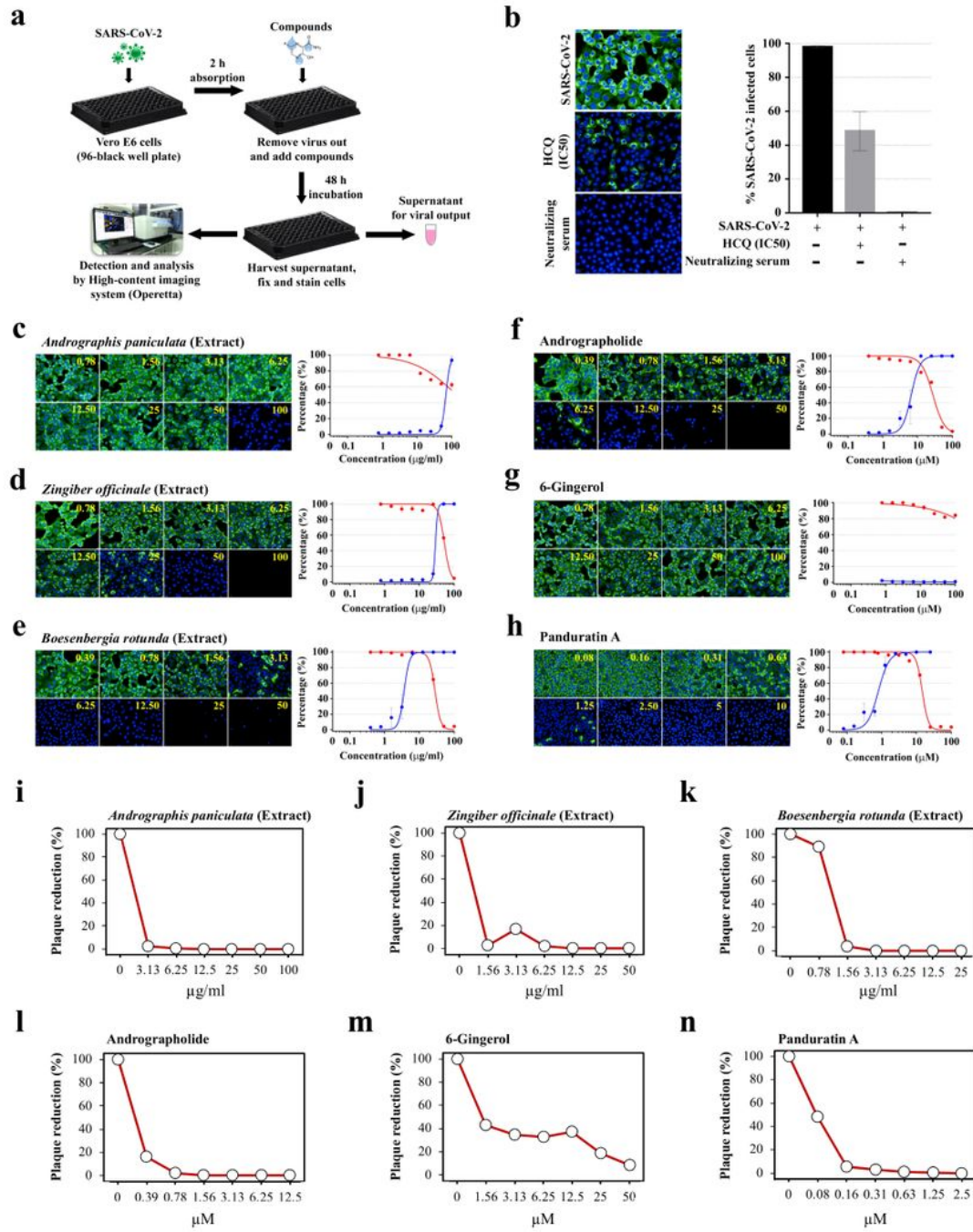


**Figure 2**

Dose-dependent anti-SARS-CoV-2 effects of six candidates at the post-infectious phase. (a). Study design. SARS-CoV-2 infected Vero E6 cells (at 25TCID<sub>50</sub>) were treated with the extract/compound for 48 hrs before harvest. (b). Controls. Hydroxychloroquine (HCQ) at the IC50 (5.08  $\mu\text{M}$ ) for post-infection

treatment (from Figure 1c) and the neutralizing serum served as the positive controls. (c-h). High-content imaging analysis of Andrographis paniculata extract (c), Zingiber officinale extract (d), Boesenbergia rotunda extract (e), Andrographolide (f), 6-Gingerol (g), and Panduratin A (h) were demonstrated in the left panel, and the %inhibition (red) and %cytotoxic (blue) showed in the right panel ( $n=3$  biological replicates). Fluorescent signals: green, anti-SARS-CoV-2 NP mAb; blue, Hoechst. (i-n). Plaque reduction assay of six candidates, i.e., *A. paniculata* extract (i), *Z. officinale* extract (j), *B. rotunda* extract (k), Andrographolide (l), 6-Gingerol (m), and Panduratin A (n) ( $n=2$  biological replicates).

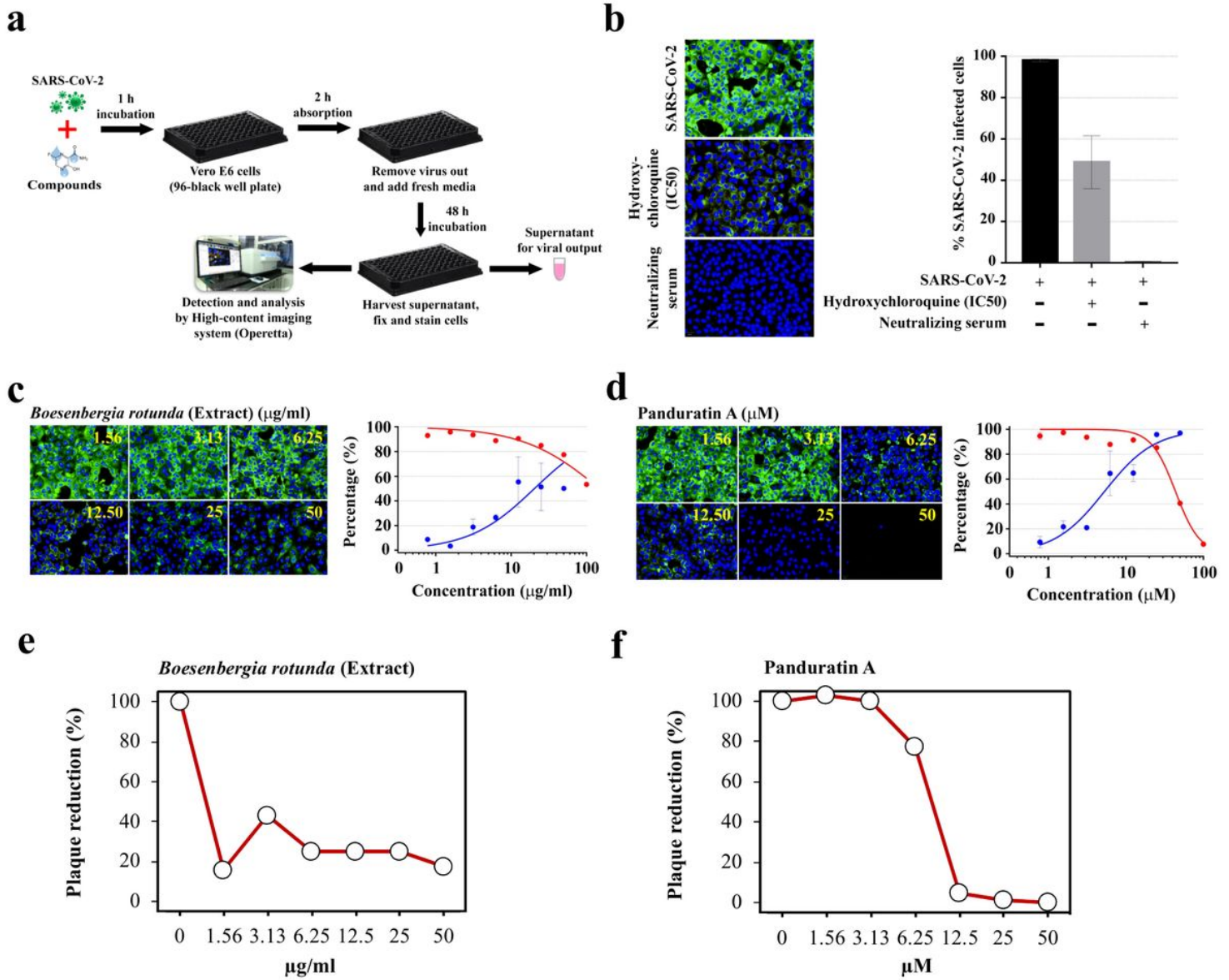


**Figure 3**

Dose-dependent anti-SARS-CoV-2 effects of *B. rotunda* extract and panduratin A at the entry phase. (a). Study design. SARS-CoV-2 at 25TCID<sub>50</sub> were incubated with the extract/compound for 1 hr before inoculation into Vero E6 cells. Viral adsorption was allowed for 2 hrs in the presence of the

extract/compound. After washing, the culture was maintained in fresh media for 48 hrs before harvest. (b). Controls. Hydroxychloroquine (HCQ) at the IC50 (8.07  $\mu$ M) for pre-entry treatment (details in Supplementary Figure 1) and the neutralizing serum served as the positive controls (n=3 biological replicates). (c-d). High-content imaging analysis of Boesenbergia rotunda extract (c) and Panduratin A (d) (the left panel), and %inhibition (red) and %cytotoxicity (blue) (the right panel) (n=3 biological replicates). Fluorescent signals: green, anti-SARS-CoV-2 NP mAb; blue, Hoechst. (e-f). Plaque reduction assay of B. rotunda extract (e) and panduratin A (f).

## Supplementary Files

This is a list of supplementary files associated with this preprint. Click to download.

- [PrePrintPanASupplementaryInformation.edited.docx](#)